ISSN 0023-1584, Kinetics and Catalysis, 2009, Vol. 50, No. 6, pp. 824–829. © Pleiades Publishing, Ltd., 2009.
Original Russian Text © M.V. Bukhtiyarova, A.S. Ivanova, G.S. Litvak, L.M. Plyasova, 2009, published in Kinetika i Kataliz, 2009, Vol. 50, No. 6, pp. 858–863.

Phase Composition and Texture of Sr(La)Mn Hexaaluminates

M. V. Bukhtiyarova, A. S. Ivanova, G. S. Litvak, and L. M. Plyasova

Boreskov Institute of Catalysis, Siberian Branch, Russian Academy of Sciences, Novosibirsk, 630090 Russia
e-mail: mvb@catalysis.ru

Received October 13, 2008

Abstract—Hexaaluminates synthesized by precipitation and calcined at 700–1400°C have been characterized by atomic absorption spectroscopy, thermal analysis, X-ray powder diffraction, and adsorption methods. The heat treatment of the Mn-substituted and unsubstituted materials at 1100 and 1200°C yields a hexaaluminate phase. The specific surface area of the samples calcined at 1100°C is 20–49 m^2/g. The texture of the samples calcined at 1000°C is characterized by a unimodal mesoporous pore size distribution with a mean pore diameter of 290 Å.

DOI: 10.1134/S0023158409060056

In recent years, there has been marked progress in hydrocarbon oxidation processes in the presence of thermally stable catalysts [1, 2]. These processes are used in many industrial applications, such as catalytic combustion chambers and catalytic afterburners of exhaust gases [3]. In addition, hexaaluminates have recently found application in N_2O decomposition [4]. Among the oxide compositions, hexaaluminate-based systems with the general formula $Sr(La)Mn_xAl_{12-x}O_{19}$ are thermally very stable and show high catalytic activity. Their high thermal stability is due to their unique layered structure, which is built of Al_2O_3 spinel blocks situated between large cations (Ba, Sr, La, etc.) located in the plane of symmetry [5]. The microstructure of materials, including ceramics, depends on the synthesis conditions and heat treatment temperature and, accordingly, the presence of other phases [6]. It is, therefore, pertinent to study the effect of admixed components on the formation of the physicochemical properties of hexaaluminates.

Here, we report the synthesis of $Sr(La)Mn_xAl_{12-x}O_{19}$ ($x = 0$; 2) and the effects of the nature of the alkali, rare-earth, and transition elements on the structure and texture of the hexaaluminates.

EXPERIMENTAL

Hexaaluminates were precipitated from solutions of metal (Al, Sr, La, Mn) nitrates by adding a concentrated aqueous solution of NH_4HCO_3 at pH 7.5–8.0 and $T = 70$°C, and the precipitate was aged under the same conditions for 2 h [5, 7]. The resulting solid was filtered, washed, and dried in air at ambient temperature and then at 110°C for 12 h. The dry solids were calcined at 700°C in flowing dry air for 4 h and were then calcined at 1100, 1200, and 1400°C in a muffle furnace for 4 h.

The products were analyzed for their main components by atomic absorption spectrometry [8] with an accuracy of 0.01–0.03%.

Differential thermal analysis (DTA) was carried out in air between 20 and 1400°C using a Netzsch STA 449 thermoanalytical system (heating rate of 10 K/min, sample size of 70 mg). The accuracy of weight loss measurements was ±0.5%.

X-ray powder diffraction patterns were obtained on a D-500 diffractometer (monochromated CuK_α radiation, $\lambda = 1.5418$ Å; 2θ scanning between 10° and 75° with 0.05° increments; counting time of 5 s per point). Phase analysis was performed by comparing the calculated interplanar spacings d_i and the corresponding reflection intensities I_i with the theoretical values presented in the JCPDS database (PCPDF, Win. Ver. 1.30, JCPDS ICDD, Swarthmore, Pa., United States, 1997).

Specific surface areas (S_{BET}) were determined by thermal argon desorption with an error of ±10% [9]. Texture properties were derived from low-temperature (–196°C) nitrogen adsorption isotherms obtained using an ASAP-2400 instrument (Micromeritics).

RESULTS AND DISCUSSION

The experimental percentages of the main components in the hexaaluminates, determined by chemical analysis, differ from the corresponding theoretical values, but the difference is insignificant. From these data, we derived the chemical formulas of the hexaaluminates (Table 1).

Nonisothermal, temperature-programmed heat treatment of the initial air-dry samples gives rise to endothermic and exothermic peaks in the DTA

Table 1. Chemical composition of hexaaluminates

Catalyst	SrO	La_2O_3	Mn_2O_3	Al_2O_3	Composition (experimental)
	mol % (calculated)				
1, $SrAl_{12}O_{19}$	14.3	–	–	85.7	$Sr_{0.86}Al_{12}O_{18.9}$
2, $LaAl_{11}O_{18}$	–	8.3	–	91.7	$La_{0.87}Al_{11}O_{17.8}$
3, $SrMn_2Al_{10}O_{19}$	14.3	–	14.3	71.4	$Sr_{0.67}Mn_{2.28}Al_{10}O_{19.09}$
4, $Sr_{0.8}La_{0.2}Mn_2Al_{10}O_{19}$	11.6	1.4	14.5	72.5	$Sr_{0.69}La_{0.33}Mn_{2.23}Al_{10}O_{19.53}$
5, $LaMn_2Al_9O_{18}$	–	8.3	16.7	75.0	$La_{1.69}Mn_{2.43}Al_9O_{19.09}$

curves. The endotherms at $T = 140–160°C$ are due to the release of physically adsorbed water. For the manganese-free compounds $SrAl_{12}O_{19}$ and $LaAl_{11}O_{18}$, exotherms occur above 900°C, which are due to the crystallization of $SrAl_2O_4$ and $LaAlO_3$ (Fig. 1a). For the substituted hexaaluminates, only endotherms are observed between 260 and 950°C, which can be assigned to carbonate decomposition (Fig. 1b).

Manganese carbonate begins to decompose at 100°C, its complete decomposition to MnO takes place at 375–450°C, and strontium carbonate decomposes to SrO at 1150°C [10]. Therefore, the endotherms at 259 and 433°C (Fig. 1b) are assignable to manganese carbonate decomposition. It is likely that this process is accompanied by the oxidation of the resulting MnO to Mn_2O_3 [11]. This is suggested by the endotherm at 602°C and by the slight weight gain (Δm) indicated by the TG curve between 600 and 700°C. The endotherm at 950°C is apparently due to strontium carbonate decomposition. The fact that the observed strontium carbonate decomposition temperature is lower than that reported in the literature [12] is possibly explained by the presence of manganese in the sample.

The crystallization of substituted and unsubstituted hexaaluminates begins at 1100 and 1200°C, respectively [5, 13], which is in agreement with X-ray diffraction data. According to these data, the hexaaluminates calcined at 700°C are X-ray-amorphous. Heat treatment of the unsubstituted hexaaluminates $SrAl_{12}O_{19}$ and $LaAl_{11}O_{18}$ at 1000°C changes their phase composition, yielding trace amounts of $SrAl_2O_4$ and Al_2O_3 (Fig. 2, Table 2). For $SrAl_{12}O_{19}$, raising the heat-treatment temperature to 1200°C favors the formation of a single-phase hexaaluminate; in the case of $LaAl_{11}O_{18}$, the product contains a perovskite phase along with the hexaaluminate phase. Therefore, replacing the alkaline-earth element with a rare-earth element in the hexaaluminate structure retards the crystallization of the hexaaluminate phase.

Both phases persist upon the heat treatment of the La-containing sample at 1400°C. However, an analysis of peak intensities suggests that the proportion of the perovskite phase in the resulting material is smaller and the proportion of the hexaaluminate phase is larger (Fig. 2b). Therefore, obtaining the pure hexaaluminate phase in the La–Al–O systems is possible either by raising the heat treatment temperature or by extending the heat treatment at a fixed temperature.

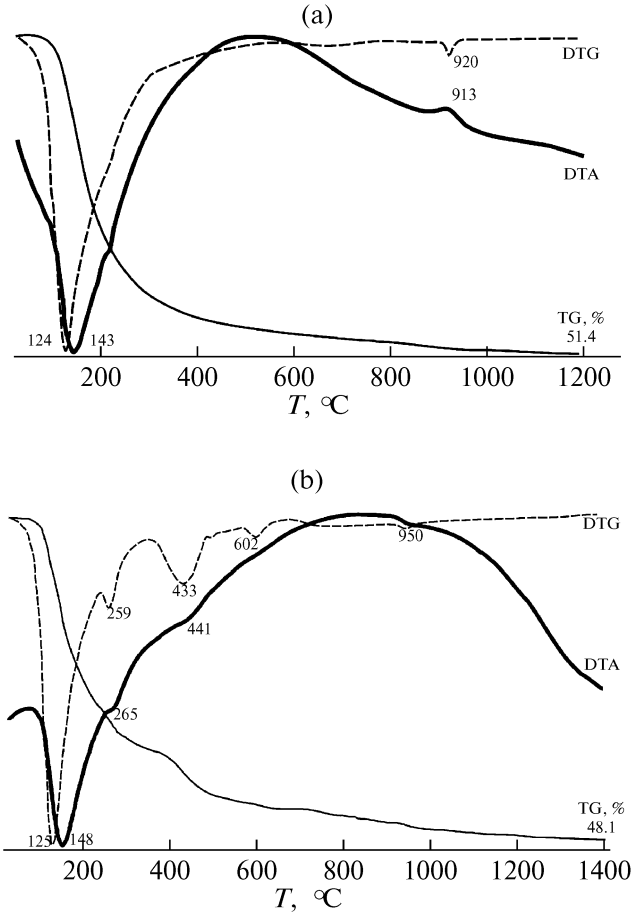

Fig. 1. Typical thermoanalytical curves of air-dry (a) $SrAl_{12}O_{19}$ and (b) $SrMn_2Al_{10}O_{19}$.

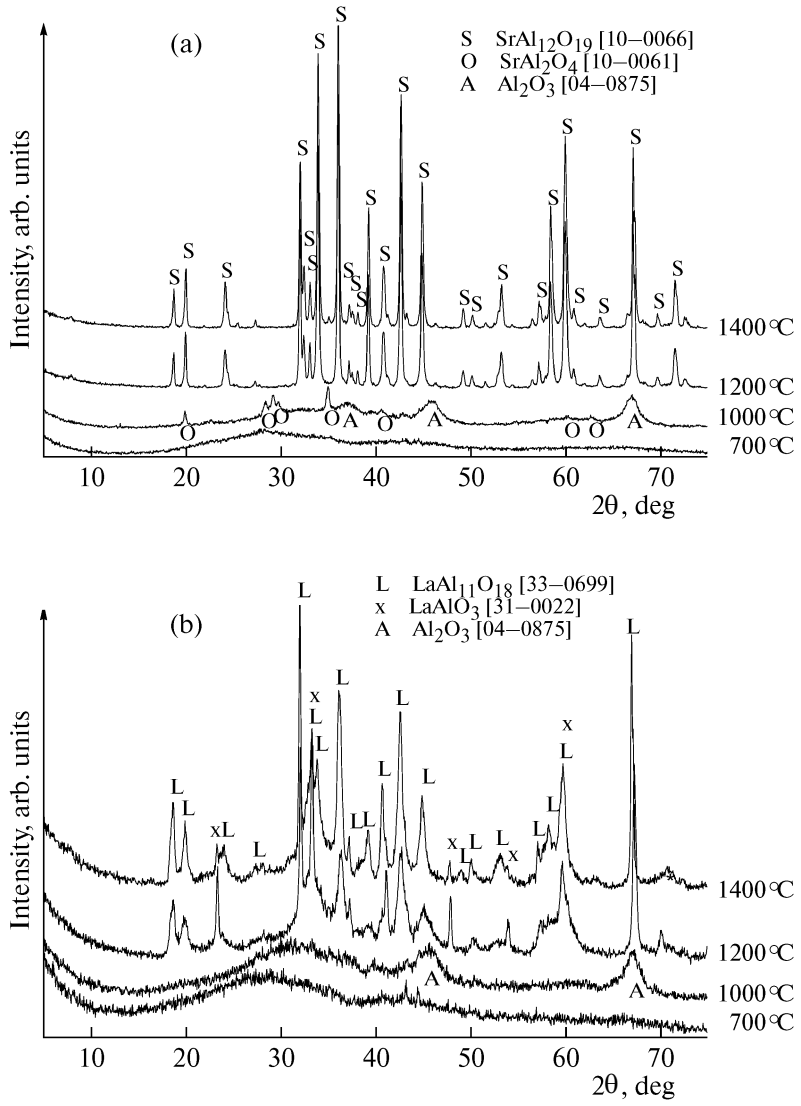

Fig. 2. X-ray diffraction patterns from (a) $SrAl_{12}O_{19}$ and $LaAl_{11}O_{18}$ (b) calcined at 700–1400°C.

In substituted samples, the hexaaluminate phase forms upon heat treatment at 1100°C (Table 2). The amounts of impurity phases were determined by comparing the observed diffraction peak profiles to the corresponding theoretical profiles using the PCW program [14, 15]. Figure 3a shows the diffraction pattern from $SrMn_2Al_{12}O_{19}$ calcined at 1100°C. Clearly, this sample consists largely of the hexaaluminate phase and contains $MnAl_2O_4$, Mn_3O_4, and α-Al_2O_3 (Fig. 3a). These minor phases survive heat treatment at 1400°C, but their proportion in the resulting sample is smaller, while the proportion of the hexaaluminate is larger (Fig. 3b).

The main phase in $Sr_{0.8}La_{0.2}Mn_2Al_{12}O_{19}$ and $LaMn_2Al_9O_{18}$ calcined at 1100°C is again hexaaluminate. The impurity phases are $LaMnO_3$, $Sr_2Mn_2O_5$, and $SrMn_3O_6$ in the Sr–La–Mn sample and $LaAlO_3$ and Mn_3O_4 (traces) in the La–Mn sample. Raising the heat treatment temperature to 1400°C alters the phase composition of some materials: in $Sr_{0.8}La_{0.2}Mn_2Al_{12}O_{19}$, the $Sr_2Mn_2O_5$ and $SrMn_3O_6$ phases are not observed at this temperature and the phase Mn_3O_4 appears; in $LaMn_2Al_9O_{18}$, Mn_3O_4 is replaced by $MnAl_2O_4$ (Table 2).

Thus, the materials in question are X-ray-amorphous at $T \leq 700$°C. The unsubstituted hexaaluminates at $T = 1000$°C contain the $SrAl_2O_4$ and $LaAlO_3$ phases; at $T \geq 1200$°C, the strontium sample is pure hexaaluminate and $LaAl_{11}O_{18}$ additionally contains a minor amount of a perovskite phase. The Mn-substituted samples ($T \geq 1100$°C) are multiphase, dominated by the hexaaluminate phase. Therefore, the introduction of manganese shifts the hexaaluminate crystallization point to lower temperatures.

Table 2. Phase composition of hexaaluminates

Sample	Phase composition			
	1100°C, 4 h		1400°C, 4 h	
	phase	a, b, c, Å	phase	a, b, c, Å
1	$SrAl_{12}O_{19}^{*}$	$a = 5.568$, $c = 22.06$	$SrAl_{12}O_{19}$	$a = 5.572$, $c = 22.03$
2	$LaAl_{11}O_{18}^{*}$	$a = 5.590$, $c = 22.18$	$LaAl_{11}O_{18}$	$a = 5.607$, $c = 21.65$
	$LaAlO_3$		$LaAlO_3$	
3	$SrAl_{12}O_{19}$	$a = 5.644$, $c = 22.522$	$SrAl_{12}O_{19}$	$a = 5.644$, $c = 22.236$
	Mn_3O_4	$a = 5.762$, $c = 9.439$	Mn_3O_4	$a = 5.762$, $c = 9.439$
	$MnAl_2O_4$	$a = 8.290$	$MnAl_2O_4$	$a = 8.290$
	α-Al_2O_3	$a = 4.759$, $c = 12.992$	α-Al_2O_3	$a = 4.759$, $c = 12.992$
4	$SrAl_{12}O_{19}$	$a = 5.588$, $c = 22.110$	$SrAl_{12}O_{19}$	$a = 5.604$, $c = 22.110$
	$LaMnO_3$	$a = 5.896$, $b = 7.652$, $c = 5.592$	$LaMnO_3$	$a = 5.862$, $b = 7.652$, $c = 5.592$
	$Sr_2Mn_2O_5$	$a = 5.531$, $b = 10.783$, $c = 3.814$	Mn_3O_4	$a = 8.290$
	$SrMn_3O_6$	Not determined		
5	$LaMnAl_{11}O_{19}$	$a = 5.616$, $c = 22.12$	$LaMnAl_{11}O_{19}$	$a = 5.616$, $c = 22.12$
	$LaAlO_3$	$a = 5.370$, $c = 13.108$	$LaAlO_3$	$a = 5.370$, $c = 13.108$
	Mn_3O_4	$a = 5.762$, $c = 9.439$	$MnAl_2O_4$	$a = 8.290$

* 1200°C.

The specific surface area of the hexaaluminates is determined by the nature and proportions of their components and by the heat treatment temperature. The S_{BET} value of the dry samples varies between 66 and 112 m^2/g. Raising the heat treatment temperature to 700°C for both substituted and unsubstituted samples does not cause any significant changes in S_{BET} (Table 3), and only heat treatment at 1100 and 1200°C, respectively, sharply reduces their S_{BET}, irrespective of their elemental composition. According to X-ray diffraction data, phase crystallization occurs at these temperatures, possibly accompanied by sintering. The specific surface area of the samples calcined at 1100 or 1200°C is 16–28 m^2/g, except for $SrMn_2Al_{10}O_{19}$, whose S_{BET} is ~2 times larger.

Among the materials considered here, $LaAl_{11}O_{18}$ and $SrMn_2Al_{11}O_{19}$ show higher thermal stability, and the Mn-substituted hexaaluminate is thermally more stable than the unsubstituted one. Thus, the introduction of manganese affords more disperse and more heat-resistant hexaaluminates. The observed difference between the thermal stabilities of these materials is likely due to the fact that $SrMn_2Al_{11}O_{19}$ contains a larger number of phases, which retards sintering, and has a persistent porous structure.

By way of example, we report the texture parameters of strontium aluminate calcined at 700, 1000, and 1200°C for 4 h. The sample calcined at 700°C has a biporous texture with a pore diameter of 200–750 Å (Fig. 4a), and the mean pore diameter is 302 Å. Raising the heat treatment temperature to 1000°C yields a nearly unimodal mesoporous material (Fig. 4a) with a mean pore diameter of 290 Å. These data suggest that the thermal stability of the above materials is due to the

Table 3. Specific surface area of hexaaluminates

Sample	S_{BET}, m^2/g		
	110°C	700°C	1100°C (1200°C)
$SrAl_{12}O_{19}$	112	121	(18)
$LaAl_{11}O_{18}$	66	74	(22)
$SrMn_2Al_{10}O_{19}$	106	145	49
$Sr_{0.8}La_{0.2}Mn_2Al_{10}O_{19}$	73	87	23
$LaMn_2Al_9O_{18}$	80	86	21

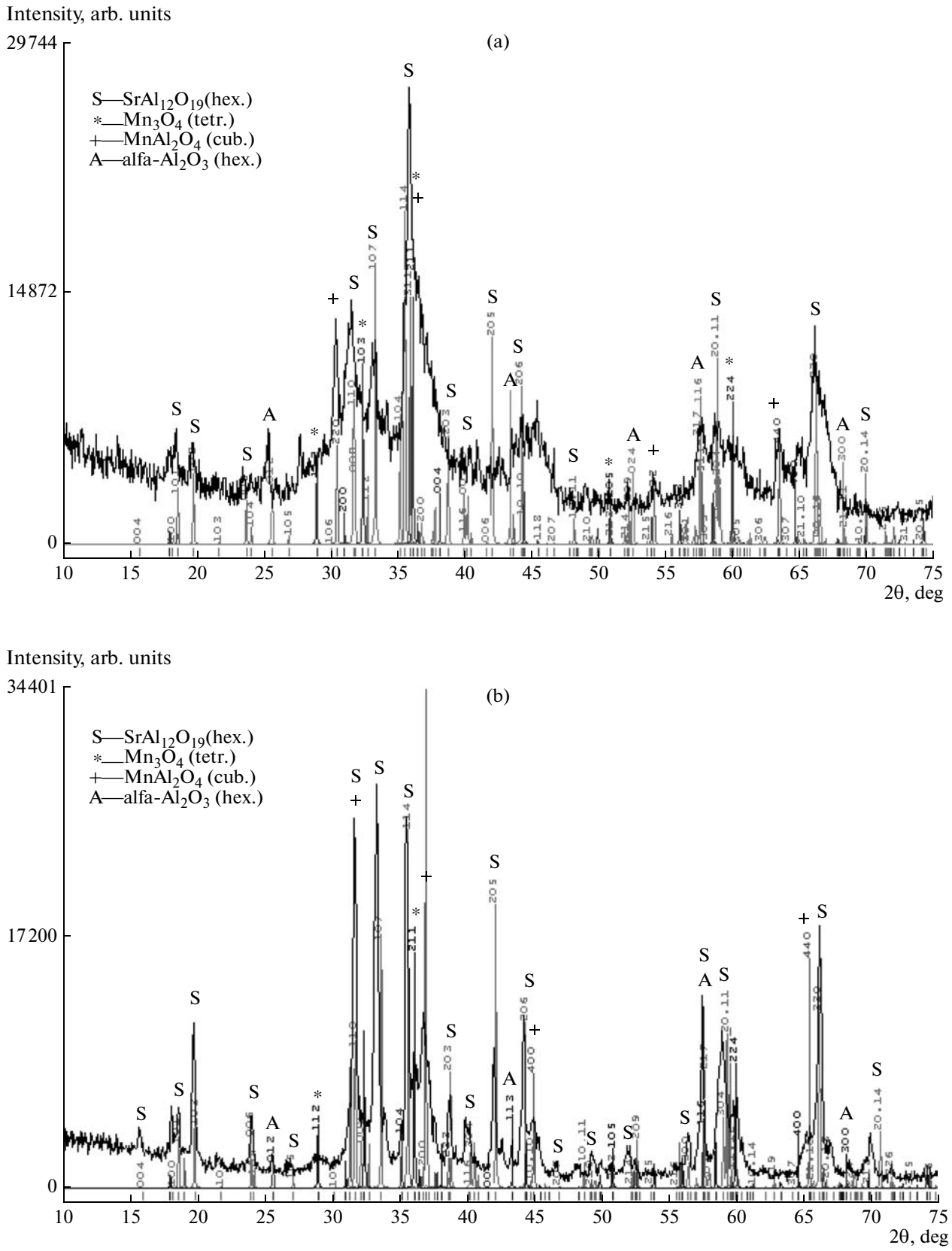

Fig. 3. X-ray diffraction patterns from $SrMn_2Al_{10}O_{19}$ calcined at (a) 1100 and (b) 1400°C.

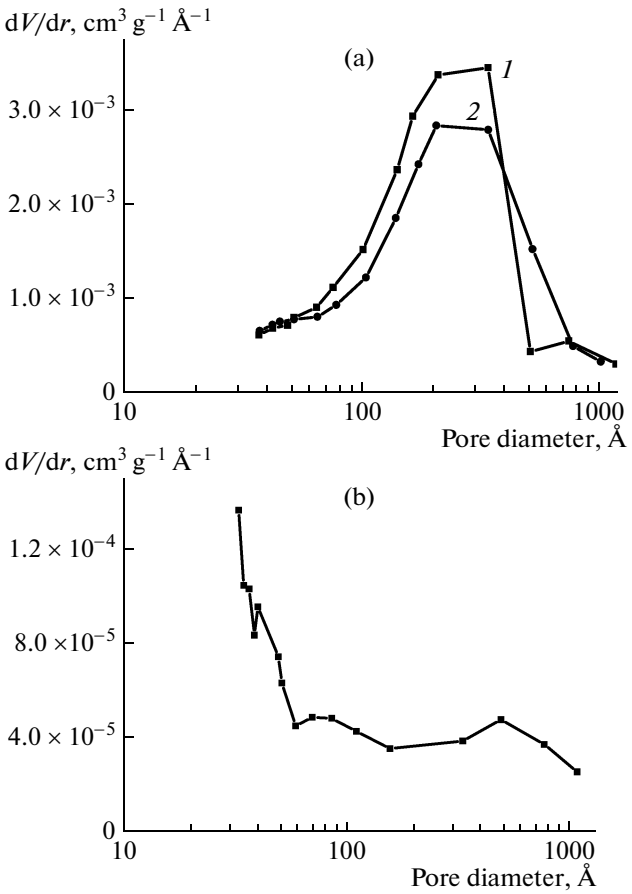

Fig. 4. Pore size distribution in $SrAl_{12}O_{19}$ calcined at (a) (*1*) 700, (*2*) 1000, and (b) 1200°C.

fact that they do not undergo bulk sintering at 1000°C, as is indicated by the constancy of the mean pore diameter. Only surface sintering takes place, resulting in a slight decrease in S_{BET} from 133 to 111 m^2/g.

The heat treatment of strontium aluminate at 1200°C causes radical textural changes: the pore size distribution changes from unimodal mesoporous to polydisperse (Fig. 4b), and the pore volume and the mean pore diameter decrease dramatically. These textural changes are due to the fact that hexaaluminate crystallization is accompanied by extensive bulk sintering, which yields fine pores 30–50 Å in diameter (Fig. 4b). It is the contribution from these pores that reduces the mean pore diameter, which turns out to be 181 Å.

REFERENCES

1. Yin, F., Ji, S., Wu, P., Zhao, F., and Li, C., *J. Mol. Catal. A: Chem.*, 2008, vol. 294, nos. 1–2, p. 27.
2. Kikuchi, R., Iwasa, Y., Takeguchi, T., and Eguchi, K., *Appl. Catal., A,* 2005, vol. 281, nos. 1–2, p. 61.
3. Kikuchi, R., Tanaka, Yo., Sasaki, K., and Eguchi, K., *Catal. Today*, 2003, vol. 83, nos. 1–4, p. 223.
4. Zhu, S., Wang, X., Wang, A., and Zhang, T., *Catal. Today*, 2008, vol. 131, nos. 1–4, p. 339.
5. Groppi, G., Cristiani, C., and Forzatti, P., *Appl. Catal., B*, 2001, vol. 35, no. 2, p. 137.
6. Vishista, K. and Gnanam, F.D., *J. Eur. Ceram. Soc.*, 2009, vol. 29, no. 1, p. 77.
7. Lietti, L., Cristiani, C., Groppi, G., and Forzatti, P., *Catal. Today*, 2000, vol. 59, nos. 1–2, p. 191.
8. Price, W., *Analytical Atomic Absorption Spectroscopy*, New York: Wiley-Interscience, 1972.
9. Buyanova, N.E., Karnaukhov, A.P., and Alabuzhev, Yu.A., *Opredelenie poverkhnosti dispersnykh i poristykh materialov* (Determination of the Surface Area of Disperse and Porous Materials), Novosibirsk: Inst. Kataliza, 1978, p. 74.
10. Nekrasov, V.V., *Osnovy obshchei khimii* (Fundamentals of General Chemistry), Moscow: Khimiya, 1973, vol. 1, p. 656.
11. Remy, H., *Lehrbuch der anorganischen Chemie*, Leipzig: Akademische, 1955, vol. 2.
12. Remy, H., *Lehrbuch der anorganischen Chemie*, Leipzig: Akademische, 1955, vol. 1.
13. Yan, L. and Thompson, L.T., *Appl. Catal., A*, 1998, vol. 171, no. 2, p. 219.
14. Kraus, W. and Nolze, G., *CPD Newsletter*, 1998, no. 20, p. 27.
15. Solov'eva, L.P., Tsybulya, S.V., and Zabolotnyi, V.A., *Polikristall – sistema programm dlya strukturnykh raschetov* (Polikristall: Software Package for Structure Calculations), Novosibirsk: Inst. Kataliza, 1988, p. 122.